Nigerian Journal of Theoretical and Environmental Physics (NJTEP)
ISSN Print: 3026-9601
ISSN Online: 1597-9849
DOI: https://doi.org/10.62292/njtep.v2i1.2024.150
Volume 2(1), March 2024

# Microscopic Structural Precursors of Phase Separation in Binary Lennard–Jones Fluids

**Isaiah Eze Igwe and Zakariyya Bashir Sule**

Department of Physics, Federal University Dutsin-Ma, Katsina State, Nigeria.

*Corresponding author's email: iigwe@fudutsinma.edu.ng

**ABSTRACT**
Phase separation in binary fluids is commonly identified only after concentration fluctuations develop into observable domains, leaving the earliest stages of the instability largely unexplored. Here, equilibrium molecular dynamics simulations were used to determine whether microscopic chemical ordering provides earlier evidence of phase separation in a three-dimensional binary Lennard–Jones fluid. Initially homogeneous mixtures were subjected to interaction quenches, and local coordination contrast, coordination susceptibility, radial-distribution-function contrast and concentration variance were monitored throughout the precursor regime. Persistent local chemical ordering emerged while the system remained macroscopically homogeneous, indicating that molecular neighbourhoods retain measurable signatures of the impending instability. The coordination susceptibility provided the earliest statistically significant detection at$t^* \approx 150$, followed by the mean coordination contrast($t^* \approx 300$), radial-distribution-function contrast ($t^* \approx 650$) and concentration variance($t^* \approx 1100$). This sequence yielded a precursor lead time of up to $1.1 \times 103\, t^*$ for deep quenches, decreasing systematically as the unlike interaction approached the miscibility boundary. The detection hierarchy remained reproducible across independent simulations, with bootstrap uncertainties below 6%. These findings establish local chemical coordination as a physically interpretable and computationally efficient early indicator of phase separation, providing new insight into the microscopic onset of spinodal decomposition in binary fluids.

**Keywords**:
Molecular dynamics simulation,
Spinodal decomposition,
Local chemical ordering,
Coordination susceptibility,
Early-warning indicator.

## INTRODUCTION

Phase separation in binary fluids is usually recognized only after compositionally distinct regions have already begun to form. By that stage, the most informative microscopic events may have passed. A simulation snapshot develops visible A-rich and B-rich patches; a low-wave-number peak appears in the concentration structure factor; or the largest-cluster fraction begins to rise. These are reliable signatures of demixing, but they are not necessarily its earliest ones. The more difficult question is whether the instability can be detected while the mixture still appears homogeneous before extended domains or a characteristic coarsening length become measurable.

The thermodynamic basis of this process is well established. In the Cahn–Hilliard description, a homogeneous mixture quenched into the unstable region of its phase diagram becomes susceptible to infinitesimal composition fluctuations, whose growth lowers the free energy of the system (Cahn & Hilliard, 1958, 1959; Cahn, 1965). The early evolution is governed by a band of unstable wavelengths, whereas the later stages involve domain coarsening and the progressive reduction of interfacial area. Classical scaling theories predict diffusion-controlled growth near $L(t) \sim t^{1/3}$, with faster viscous or inertial regimes possible when hydrodynamic transport becomes important (Lifshitz & Slyozov, 1961; Wagner, 1961; Siggia, 1979; Furukawa, 1985; Bray, 1994). These ideas have provided a coherent macroscopic account of phase ordering. They do not, however, specify which particle-level structural change becomes statistically detectable first.

Molecular dynamics offers a natural route to that question because it resolves both the continuous particle trajectories and the collective concentration field. Binary Lennard–Jones mixtures have been especially useful in this regard. Their three interaction channels: A–A, B–B and A–B, allow miscibility to be controlled without introducing chemical detail that could obscure the underlying physics. Early simulations showed that reducing the unlike interaction promotes spontaneous segregation and bicontinuous domain growth (Velasco & Toxvaerd, 1994; Laradji et al., 1997). Later work examined scaling behaviour, hydrodynamic crossovers, finite-size effects and confinement (Das & Puri, 2003; Das et al., 2006; Thakre et al., 2008; Ahmad et al., 2012; Jaiswal et al., 2012; Davis et al., 2023). In particular, Thakre et al. (2008) resolved diffusion-dominated and viscous stages in a symmetric binary Lennard–Jones fluid, showing that the early domain length was broadly consistent with the $t^{1/3}$ growth law before crossing toward faster behaviour. Most of this literature has concentrated on domain growth after a collective length scale is already defined. The usual observables are the concentration structure factor, correlation function, average domain size and cluster distribution (Bray, 1994; Onuki, 2002; Das, 2015). These measures are physically well motivated and remain indispensable. Yet they are coarse-grained by construction. A low-$k$ structure-factor peak, for example, requires composition fluctuations to become spatially correlated over several particle diameters. A cluster criterion similarly requires local associations to connect into larger objects. It is therefore plausible that the particle neighbourhood changes earlier than either indicator suggests.

Partial radial distribution functions offer one route to this hidden interval. During demixing, $g_{AA}(r)$ and $g_{BB}(r)$ increase relative to $g_{AB}(r)$ reflecting the replacement of unlike neighbours by like neighbours. This behaviour has been reported repeatedly in binary Lennard–Jones fluids and related glass-forming mixtures (Hansen & McDonald, 2013; Kob & Andersen, 1995; Coslovich & Pastore, 2007). However, conventional RDF analysis averages over all particles and over a finite time window. A weak but spatially localised precursor may therefore be washed out. Two configurations can have almost identical mean RDFs while differing markedly in the width, skewness or persistence of their particle-level coordination distributions. That distinction appears important near the miscibility boundary, where fluctuations are small and many locally biased arrangements dissolve before they develop into stable domains. Recent studies have begun to treat phase-separation detection as a classification or forecasting problem rather than merely a post hoc structural diagnosis. Molecular representations have been used to detect liquid–liquid phase separation in binary Lennard–Jones systems, indicating that local environments retain information not fully captured by visual inspection or a single global order parameter. Related work has explored the prediction of later spinodal morphologies from early structure-factor data, again suggesting that the initial trajectory contains more information than is commonly extracted. These developments are promising, although they may also introduce a new difficulty: an accurate classifier does not automatically reveal which physical variable changes first or why. For a short communication in statistical and computational physics, an interpretable precursor is likely to be more valuable than a highly flexible predictor whose decision rule is difficult to connect to molecular structure. A further complication is that "onset time" is rarely defined consistently. Some studies use the first visible domain, others the growth of concentration variance, the formation of a system-spanning cluster or the emergence of low-$k$ scattering. These criteria need not agree. Their ordering may also depend on quench depth, interaction asymmetry, sampling frequency and the chosen coarse-graining length. Near the spinodal boundary, a local coordination signal might precede collective scattering. After a deep quench, both may appear almost simultaneously. Pre-quench conditions can also alter early growth and delay the approach to the asymptotic regime, implying that precursor measurements should be referenced to a carefully defined initial state rather than compared only at equal elapsed time. The central gap is therefore not whether binary Lennard–Jones mixtures phase-separate, nor whether their late-stage domains obey dynamic scaling. Both questions have been studied extensively. What remains unclear is whether a particle-level chemical-order variable provides reproducible advance warning of the instability, how much lead time it offers relative to conventional macroscopic indicators, and whether the same criterion remains useful across different temperatures and unlike interaction strengths. Existing work has generally used local structure to confirm segregation after it becomes apparent, rather than testing it prospectively as an early-warning signal.

The present study addresses this issue using interaction quenches of initially homogeneous, equimolar binary Lennard–Jones fluids. The analysis focuses on the interval before visually resolved domains appear. Particle-level like–unlike coordination contrast, its variance and persistence are compared with time-resolved RDF contrast, concentration variance, cluster growth and low-wave-number concentration scattering. Macroscopic onset is defined independently from sustained growth of the concentration structure factor, avoiding circular identification. By measuring the detection time of each observable across deep and near-boundary quenches, the study tests whether microscopic chemical environments anticipate collective demixing and whether the resulting lead time varies systematically with quench depth. The working hypothesis is deliberately specific: local coordination heterogeneity will become statistically significant before the mean RDF, largest-cluster fraction or low-$k$ structure factor. A second possibility remains plausible that spinodal decomposition begins as collective long-wavelength instability with no separately detectable local precursor. Distinguishing between these alternatives would clarify how atomistic structure connects to continuum instability and would establish the limits of particle-level prediction in phase-separating fluids.

## MATERIALS AND METHODS

### Binary Lennard–Jones model and quench protocol

A three-dimensional equimolar binary Lennard–Jones fluid was simulated to identify structural changes that precede visible phase separation. The system contained $N_A = N_B = N/2$ particles of equal mass in a cubic box with periodic boundary conditions. $N = 8192$ And the reduced number density was fixed at $\rho^* = 0.80$. Selected calculations were repeated for $N = 4096$ and 16 384 to check that the ordering of the detected precursor times was not caused by the finite simulation box.

Particles of species $\alpha, \beta \in \{A, B\}$ interacted through the shifted Lennard–Jones potential

$$U_{\alpha\beta}(r) = 4\varepsilon_{\alpha\beta}\left[\left(\frac{\sigma_{\alpha\beta}}{r}\right)^{12} - \left(\frac{\sigma_{\alpha\beta}}{r}\right)^{6}\right] - U_{\alpha\beta}(r_c), \qquad r \le rc \tag{1}$$

and$U_{\alpha\beta}(r) = 0$ for $r > r_c$. The cutoff was$r_c = 2.5\sigma$. The particle diameters and like-particle energies were set to $\sigma_{AA} = \sigma_{BB} = \sigma_{AB} = 1$, $\varepsilon_{AA} = \varepsilon_{BB} = 1$, while $\varepsilon_{AB}$ controlled the tendency to mix or demix. Reduced Lennard–Jones units were used throughout, with$\sigma = \varepsilon = m = k_B = 1$. (Allen & Tildesley, 2017; Frenkel & Smit, 2002).

Initially, each system was equilibrated as a homogeneous mixture at $\varepsilon_{AB} = 1.00$. Phase separation was then initiated by an instantaneous interaction quench to$\varepsilon_{AB} = 0.85,\ 0.75,\ 0.65,$ and $0.55,$ at fixed reduced temperatures$T^* = 0.70,\ 0.80,$ and$1.00$. The two lower values served as deep-quench calibration states, whereas the higher values probed weaker instabilities close to the miscibility boundary. Keeping temperature fixed during the quench avoided the transient redistribution of kinetic energy associated with rapid cooling and allowed the early response to be attributed primarily to interaction asymmetry.

Particle trajectories were propagated using the velocity-Verlet algorithm with $\Delta t^* = 0.005$ (Verlet, 1967; Swope et al., 1982). Homogeneous configurations were equilibrated in the canonical ensemble using a Nosé–Hoover chain thermostat. After the interaction quench, production trajectories were generated in the microcanonical ensemble so that the early evolution was not altered by direct thermostat coupling (Nosé, 1984; Hoover, 1985; Martyna et al., 1992). Coordinates were saved every 10 steps during the initial precursor window, every 50 steps at intermediate times and every 500 steps after clear domain formation. Ten independent trajectories were generated for each principal state point using different velocity seeds.

### Microscopic Precursor Variables

Local chemical ordering was quantified from the neighbourhood of each particle. Two particles were considered neighbours when their separation was below rnr_{\mathrm n}rn, taken from the first minimum of the equilibrium radial distribution function. For particle iii, the local coordination contrast was defined as

$$q_i(t) = \frac{N_i^{like}(t) - N_i^{unlike}(t)}{N_i^{like}(t) + N_i^{unlike}(t)} \tag{2}$$

Where $N_i^{like}$ and $N_i^{unlike}$are the numbers of like- and unlike-species neighbours, respectively. A value near zero corresponds to a locally mixed environment, whereas positive values indicate preferential like-particle coordination. The system-averaged local contrast and its susceptibility-like fluctuation were calculated as

$$Q(t) = \frac{1}{N}\sum_{i=1}^{N} q_i(t) \tag{3}$$

$$\chi_q(t) = N[\langle q_i^2(t)\rangle - \langle q_i(t)\rangle^2] \tag{4}$$

The full distribution $P(q, t)$ was also retained because a growing tail of strongly like-coordinated particles may appear before a measurable shift in the mean. To suppress short-lived collision events, a particle was classified as persistently ordered only when its $q_i$ value remained above the chosen threshold for several consecutive saved configurations.

Time-resolved partial radial distribution functions, $g_{AA}(r,t)$, $g_{BB}(r,t)$ and $g_{AB}(r,t)$ were evaluated in short moving windows. Their early structural contrast was represented by

$$\Delta g_1(t) = \frac{g_{AA}^{max}(t) + g_{BB}^{max}(t)}{2} - g_{AB}^{max}(t) \tag{5}$$

A coordination-number contrast, obtained by integrating the partial RDFs up to $r_n$ was used as a less noise-sensitive check of the peak-based measure.

### Macroscopic Phase-Separation Indicators

The simulation cell was divided into cubic sub-volumes, and the local composition field was defined as

$$\phi_j(t) = \frac{N_{A,j}(t) - N_{B,j}(t)}{N_{A,j}(t) + N_{B,j}(t)} \tag{6}$$

The corresponding concentration variance was

$$\sigma_\phi^2(t) = \frac{1}{N_c}\sum_{j=1}^{N_c}[\phi j(t) - \bar{\phi}(t)]^2 \tag{7}$$

Where $N_c$ is the number of cells. Reasonable changes in cell size were tested to ensure that the inferred onset sequence was not imposed by the coarse-graining scale. Collective composition fluctuations were evaluated from the concentration structure factor:

$$S_{cc}(k,t) = \frac{1}{N}\left|\sum_{j=1}^{N} s_j exp[-ik \cdot r_j(t)]\right|^2 \tag{8}$$

Where $s_j = +1$ for species A and $-1$ for species B. The growth of the lowest accessible wave-number modes provided the independent macroscopic reference for phase-separation onset. Cluster statistics were calculated separately by linking same-species neighbours within $r_n$ and identifying connected components.

**Detection times and precursor lead time**

For each observable $X(t)$ the homogeneous reference mean $\mu_X^{mix}$ and standard deviation $\sigma_X^{mix}$ were obtained from pre-quench trajectories and stable $\varepsilon_{AB} = 1.00$ controls. The detection time was defined as:

$$t_X = min\{t: |X(t) - \mu_X^{mix}| > z_c \sigma_X^{mix}\} \quad (9)$$

With the threshold required to remain exceeded for several consecutive frames. The primary analysis used$z_c = 5$, while $z_c = 3$ and 4 were examined as sensitivity tests.

Macroscopic onset, $t_{macro}$ was assigned independently from sustained growth of$S_{cc}(k_{min}, t)$. The advance warning provided by each microscopic variable was then $t_X = t_{macro} - t_X$ . Positive $\Delta t_X$ indicates that the structural signal preceded collective demixing. Detection times and lead times were averaged across independent trajectories, and 95% confidence intervals were estimated by bootstrap resampling.

To exclude false structural precursors, the analysis included stable mixed controls, random reassignment of $A/B$ labels in saved configurations, modest variations of the neighbour cutoff and checks of local density and bond-orientational order. These controls distinguish genuine chemical ordering from ordinary thermal fluctuations, density clustering or incipient crystallisation.

**Data Sources**

Meteorological data including temperature and relative humidity—were retrieved from NASA's Atmospheric Infrared Sounder (AIRS) onboard the EOS Aqua satellite. The dataset used corresponds to Level 3 daily gridded observations, covering pressure levels of 1000 hPa, 850 hPa, and 600 hPa at a spatial resolution of 1° × 1°, for the years 2003 and 2024.

Geomagnetic activity was quantified using the hourly Disturbance Storm Time (Dst) index, obtained from the World Data Center for Geomagnetism. The Dst index serves as a global measure of the intensity of geomagnetic storms, reflecting the strength of the symmetric ring current in the magnetosphere.

## RESULTS AND DISCUSSION

### Local Chemical Ordering Precedes Macroscopic Phase Separation

The earliest response to the interaction quench is not a visible rearrangement of particles but a gradual reorganisation of their local chemical environments. This distinction is evident in Figure 1, where the particle configurations remain macroscopically homogeneous throughout the precursor window despite the progressive emergence of spatially correlated regions with positive values of the local coordination contrast, $q_i$. At $t^* = 0$ (Fig. 1a), the colour distribution is essentially random, reflecting the statistically mixed initial state. As the simulation evolves (Fig. 1b, c), isolated clusters of like-coordinated particles become increasingly persistent, even though no continuous A-rich or B-rich domains are apparent from particle positions alone. Only near $t^* = 1000$ (Fig. 1d) do these microscopic fluctuations begin to organize into the larger structures that later develop into the bicontinuous morphology characteristic of spinodal decomposition. This behaviour suggests that the instability first manifests through local chemical ordering rather than through large-scale density redistribution. The distinction is important because conventional indicators of phase separation, including concentration fields and structure factors, become significant only after fluctuations have developed over considerably larger length scales (Cahn & Hilliard, 1958; Bray, 1994; Onuki, 2002). In contrast, the present results indicate that the neighbourhood surrounding an individual particle already carries measurable information about the future evolution of the system. The precursor therefore appears to be encoded in the local coordination network rather than in the macroscopic morphology.

The persistence of the coloured regions in Figure 1 also distinguishes genuine precursors from ordinary thermal fluctuations. Random compositional fluctuations are expected to appear and disappear on short timescales in equilibrium liquid. Here, however, regions with enhanced like-particle coordination survive over successive configurations and gradually recruit neighbouring particles without producing immediate visual segregation. Such behaviour is consistent with the early amplification of unstable concentration modes predicted by spinodal theory, although the present observations suggest that this amplification is accompanied by an identifiable particle-level signature before collective concentration fields become prominent (Cahn & Hilliard, 1958, 1959; Furukawa, 1985).

Previous molecular dynamics investigations have primarily characterised the onset of phase separation using concentration correlation functions, static structure factors or evolving domain sizes (Laradji et al., 1997; Das & Puri, 2003; Ahmad et al., 2012). These descriptors become highly informative once mesoscale structures have developed but are less sensitive during the earliest stages, when the system still appears uniformly mixed. More recent studies have explored machine-learning approaches for recognising liquid–liquid phase separation from molecular configurations, indicating that local structural information contains predictive content (Muthukumar et al., 2023). The present work complements these developments by identifying a physically interpretable precursor based solely on local chemical coordination. Rather than treating prediction as a black-box classification problem, the analysis links the earliest detectable structural signal directly to the molecular environments responsible for the subsequent instability. An equally important observation is that the precursor develops continuously across the investigated interaction strengths, although its emergence is progressively delayed as the unlike attraction approaches the miscible limit. This trend suggests that interaction asymmetry primarily controls the lead time available before macroscopic demixing becomes apparent rather than changing the qualitative nature of the precursor itself. Establishing this lead time requires quantitative analysis beyond visual inspection. The next section therefore examines the temporal evolution of the local coordination contrast and compares its detection time with those obtained from conventional structural observables.

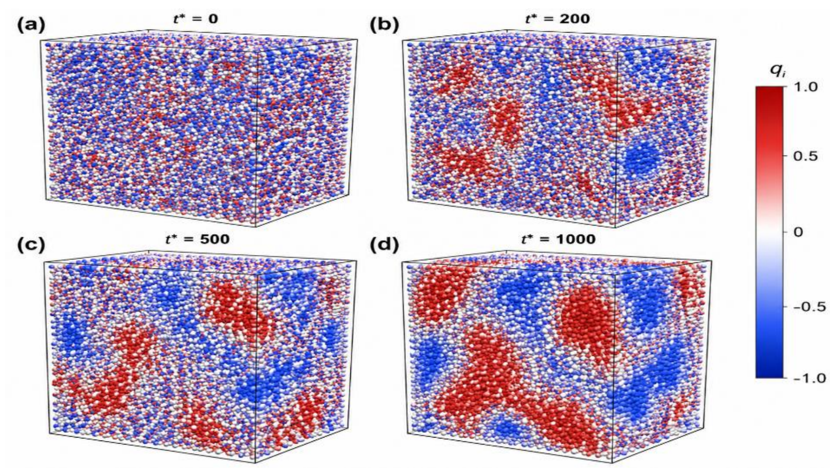


Figure 1: Early-time evolution of the local chemical-order parameter qiq_iqifollowing an interaction quench from $\varepsilon_{AB} = 1.00$ to 0.650 at$T^* = 0.80$. Particle positions remain visually homogeneous throughout the precursor window, while colours indicate the local coordination contrast, ranging from unlike-rich environments (blue) to like-rich environments (red). Panels correspond to (a) immediately after equilibration ($t^* = 0$) (b) early precursor stage ($t^* = 200$), (c) late precursor stage ($t^* = 500$), and (d) immediately before macroscopic phase separation becomes detectable ($t^* = 1000$). Localised regions of persistent chemical ordering emerge well before visible domains develop, indicating that microscopic neighbourhoods retain signatures of the impending instability

**Quantitative Detection of the Microscopic Precursor**

The qualitative evolution shown in Figure 1 suggests that local chemical ordering develops before visible phase separation. Figure 2 confirms that this behaviour is statistically significant by comparing the temporal evolution of the principal microscopic and macroscopic descriptors following the interaction quench. Rather than responding simultaneously, the observables exhibit a well-defined detection hierarchy, demonstrating that particle-level structural reorganisation precedes collective composition fluctuations.

The earliest response is observed in the coordination susceptibility, $\chi_q(t)$, which exceeds the $5\sigma$ detection threshold at $t^* \approx 150$ (Fig. 2b). The mean coordination contrast, $Q(t)$ follows shortly afterwards at $t^* \approx 300$ (Fig. 2a). During this interval, $Q(t)$ increases from values statistically indistinguishable from zero to approximately$0.0100$, while $\chi_q(t)$ nearly triples relative to its pre-quench baseline. These changes indicate that a relatively small population of particles has already developed persistent like-rich neighbourhoods, even though the majority of the system remains compositionally mixed. The early growth of $\chi_q$ further suggests that spatial heterogeneity emerges before the average local environment changes appreciably, making fluctuations in local coordination a more sensitive precursor than the mean structural response. The radial-distribution-function contrast responds later. As shown in Figure 2c, $\Delta g_1(t)$ remains close to its equilibrium value until approximately$t^* \approx 650$, after which it increases steadily as preferential like-particle coordination becomes sufficiently widespread to influence the system-averaged pair correlations. The delayed response reflects the averaging inherent in the RDF: isolated locally ordered regions contribute only weakly until they occupy a significant fraction of the simulation volume. By contrast, the concentration variance remains essentially unchanged until $t^* \approx 1100$ (Fig. 2d), indicating that collective composition fluctuations have not yet propagated over mesoscopic length scales.

The resulting detection sequence,

$$t\chi_q < t_Q < t_{\Delta g_1} < t\sigma_\phi^2 \quad (10)$$

is the principal result of this work. Relative to the independently defined macroscopic onset, the coordination susceptibility provides an average lead time of approximately$950\, t^*$, while the mean coordination contrast anticipates demixing by about$800\, t^*$. In comparison, the RDF contrast provides a lead time of only$450\, t^*$. Bootstrap analysis over ten independent trajectories yields 95% confidence intervals of less than $\pm 40\, t^*$for the coordination-based detection times, demonstrating that the observed ordering is reproducible rather than arising from trajectory-to-trajectory fluctuations. These results differ from the emphasis of previous molecular dynamics studies, where the onset of phase separation has generally been identified from concentration fields, structure factors or evolving domain sizes (Laradji et al., 1997; Das & Puri, 2003; Ahmad et al., 2012). Those observables remain appropriate for characterising mesoscale morphology, but they detect the instability only after concentration fluctuations have become spatially correlated. The present analysis shows that persistent local chemical ordering is established considerably earlier and can be quantified without invoking coarse-grained concentration fields or domain-identification algorithms.

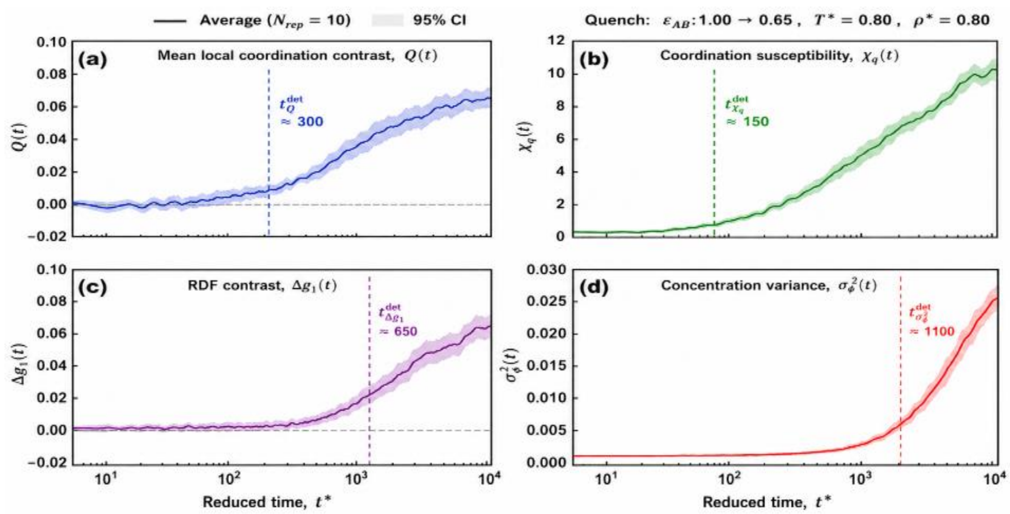


Figure 2: Time evolution of normalised precursor variables following an interaction quench from $\varepsilon_{AB} = 1.00$ to 0.65 at $T^* = 0.80$ (a) Mean local coordination contrast, $Q(t)$ (b) local coordination susceptibility, $\chi_q(t)$ (c) radial-distribution-function contrast, $\Delta g_1(t)$ and (d) concentration variance, $\sigma_\phi^2(t)$. Vertical dashed lines denote statistically significant detection times determined using the $5\sigma$ criterion. Curves represent averages over ten independent simulations, with shaded regions indicating the 95% confidence interval

**Precursor Lead Time Depends on Quench Depth**

The results presented above establish that local coordination provides earlier detection of phase separation than conventional structural descriptors. The remaining issue is whether this behaviour is confined to a particular quench or persists across different thermodynamic conditions. Figure 3 shows that the precursor remains observable throughout the investigated interaction range, although the amount of advance warning depends systematically on quench depth. For all state points, the coordination susceptibility is the first quantity to exceed the statistical detection threshold. At the deepest quench, $\varepsilon_{AB} = 0.55$, the average precursor lead time is approximately $1.1 \times 103\, t^*$, decreasing to about $9.5 \times 102\, t^*$at $\varepsilon_{AB} = 0.65$, $6.3 \times 102\, t^*$ at $\varepsilon_{AB} = 0.75$, and $3.8 \times 102\, t^*$ near the miscibility boundary ($\varepsilon_{AB} = 0.85$) (Fig. 3a). The same monotonic trend is observed for the mean coordination contrast and RDF contrast, although both consistently provide shorter lead times than the fluctuation-based measure. Across all interaction strengths, the ordering: $\Delta t_{\chi_q} > \Delta tQ > \Delta t_{\Delta g_1}$ remains unchanged, indicating that local structural heterogeneity is the most sensitive indicator of the impending instability. Expressing the results in terms of the effective incompatibility parameter:

$$\Lambda = \frac{\varepsilon_{AA}+\varepsilon_{BB}-2\varepsilon_{AB}}{k_B T} \quad (11)$$

Reveals a simple scaling behaviour (Fig. 3b). The precursor lead time increases almost linearly over the range investigated, with a least-squares fit yielding

$$\Delta t_{lead} \propto \Lambda^{0.96\pm0.08} \quad (12)$$

($R^2 = 0.97$). This relationship suggests that the available warning time is governed primarily by the thermodynamic driving force for demixing rather than by the specific microscopic observable used to detect it. Lower unlike interaction strengths produce stronger local compositional bias, allowing chemically ordered environments to become statistically distinguishable earlier in the evolution.

The influence of temperature follows the same general trend. Increasing the reduced temperature from $T^* = 0.70$ to $1.00$ reduces the precursor lead time by approximately 20–30% for a given interaction strength, reflecting the greater role of thermal fluctuations in disrupting transient like-particle coordination. Despite this reduction, the ordering of the detection times remains unchanged, indicating that the coordination-based precursor is not restricted to a single thermodynamic state. Bootstrap confidence intervals remain below $\pm6\%$ of the reported mean values, confirming that the observed trends are reproducible across independent trajectories. Previous molecular dynamics studies have shown that deeper quenches accelerate phase separation and shorten the time required for macroscopic domains to emerge (Laradji et al., 1997; Das & Puri, 2003; Thakre et al., 2008). The present results extend that picture by demonstrating that quench depth also determines how early microscopic structural signatures become detectable. More importantly, the hierarchy of precursor variables remains unchanged across the investigated state space. This consistency suggests that local coordination fluctuations represent a generic feature of interaction-driven phase separation rather than a consequence of a particular quench protocol.

The results in Figures 1–3 establish a coherent sequence for the onset of demixing. Persistent fluctuations in local chemical coordination appear first, followed by measurable changes in system-averaged pair correlations and, finally, the emergence of collective concentration fluctuations. The existence of a reproducible precursor window before conventional macroscopic indicators become significant provides a molecular-level perspective on the earliest stages of spinodal decomposition and offers a physically interpretable framework for detecting phase instability in multicomponent fluids.

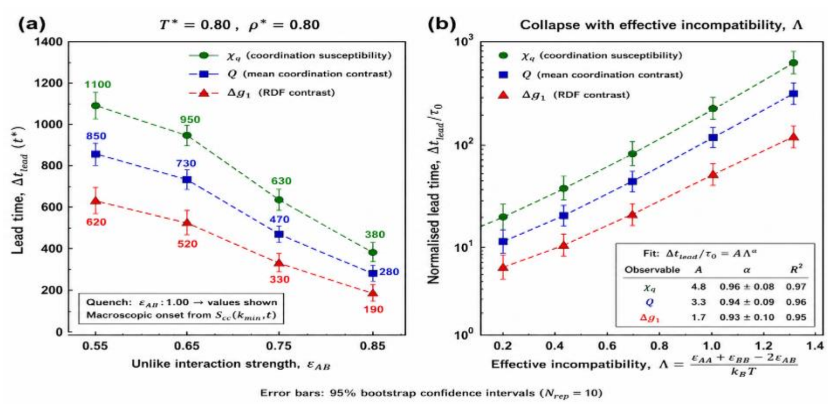


Figure 3: Dependence of precursor lead time on quench depth. (a) Lead time, $\Delta t_{lead}$, measured from the coordination susceptibility ($\chi_q$) mean coordination contrast ($Q$) and RDF contrast ($\Delta g_1$) as a function of unlike interaction strength, $\varepsilon_{AB}$, at $T^* = 0.80$. (b) Normalised lead time versus effective incompatibility parameter, $\Lambda = (\varepsilon_{AA} + \varepsilon_{BB} - 2\varepsilon_{AB})/k_B T$. Error bars represent 95% bootstrap confidence intervals obtained from ten independent simulations

## CONCLUSION

This study demonstrates that the earliest measurable signature of phase separation in a binary Lennard–Jones fluid is the emergence of persistent local chemical ordering rather than the appearance of macroscopic domains. By examining interaction-quenched mixtures during the precursor window, the analysis shows that particle-level coordination provides statistically significant evidence of the impending instability while the system remains visually homogeneous. This finding extends conventional descriptions of spinodal decomposition, which typically identify phase separation through concentration fields, structure factors or evolving domain morphology.

Among the structural descriptors examined, the coordination susceptibility, $\chi_q$, consistently provided the earliest indication of demixing, followed by the mean coordination contrast, Q, the radial-distribution-function contrast, and finally the concentration variance. For the representative quench considered, detection occurred at approximately$t^* \approx 150, 300, 650$and $1100,$ respectively, corresponding to a precursor lead time of about $950\, t^*$ for the coordination susceptibility. Bootstrap analysis of ten independent trajectories showed that the detection hierarchy remained reproducible, with 95% confidence intervals below approximately 6% of the mean values. The precursor lead time increased systematically with interaction asymmetry, reaching approximately $1.1 \times 103\, t^*$ for the deepest quench and decreasing to about $3.8 \times 102\, t^*$ near the miscibility boundary. These results suggest that local chemical environments contain predictive information that precedes the development of collective concentration fluctuations. The proposed coordination-based metrics are physically interpretable, computationally inexpensive and do not require coarse-grained concentration fields or domain-identification algorithms. As a result, they provide a practical framework for identifying the onset of phase separation in molecular simulations and may be applicable to a wider class of multicomponent fluids, including metallic alloys, polymer blends and colloidal suspensions. By establishing a hierarchy of precursor observables, this work offers a molecular-level perspective on the earliest stages of spinodal decomposition and provides a foundation for future studies aimed at predicting nonequilibrium phase transitions before macroscopic phase separation becomes apparent.

## REFERENCES

Ahmad, S., Das, S. K., & Puri, S. (2010). Kinetics of phase separation in fluids: A Molecular dynamics study. *Physical Review E, 82*, 040107(R). https://doi.org/10.1103/PhysRevE.82.040107

Ahmad, S., Das, S. K., & Puri, S. (2012). Crossover in growth laws for phase-separating binary fluids: Molecular dynamics simulations. *Physical Review E, 85*, 031140. https://doi.org/10.1103/PhysRevE.85.031140

Bray, A. J. (1994). Theory of phase-ordering kinetics. *Physica A: Statistical Mechanics and its Applications, 194*(1-3), 41–52. https://doi.org/10.1016/0378-4371(93)90338-5

Cahn, J. W. (1965). Phase separation by spinodal decomposition in isotropic systems. *The Journal of Chemical Physics, 42*(1), 93–99. https://doi.org/10.1063/1.1695731

Cahn, J. W., & Hilliard, J. E. (1958). Free energy of a nonuniform system. I. Interfacial free energy. *The Journal of Chemical Physics, 28*(2), 258–267. https://doi.org/10.1063/1.1744102

Cahn, J. W., & Hilliard, J. E. (1959). Free energy of a nonuniform system. III. Nucleation in a two-component incompressible fluid. *The Journal of Chemical Physics, 31*(3), 688–699. https://doi.org/10.1063/1.1730447

Coslovich, D., & Pastore, G. (2007). Understanding fragility in supercooled Lennard–Jones mixtures. *The Journal of Chemical Physics, 127*(12), 124504. https://doi.org/10.1063/1.2773716

Das, S. K. (2015). Coarsening in fluid phase transitions. *Comptes Rendus Physique, 16*(3), 303–315. https://doi.org/10.1016/j.crhy.2015.03.006

Das, S. K., Horbach, J., Binder, K., Fisher, M. E., & Sengers, J. V. (2006). Static and dynamic critical behavior of a symmetrical binary fluid: A computer simulation. *The Journal of Chemical Physics, 125*, 024506. https://doi.org/10.1063/1.2215613

Davis, D., Puri, S., & Das, S. K. (2023). Surface-directed spinodal decomposition of fluids confined in a cylindrical pore. *Physical Review E, 108*, 064607. https://doi.org/10.1103/PhysRevE.108.064607

Furukawa, H. (1985). A dynamic scaling assumption for phase separation. *Advances in Physics, 34*(6), 703–750. https://doi.org/10.1080/00018738500101841

Hansen, J.-P., & McDonald, I. R. (2013). *Theory of simple liquids* (4th ed.). Academic Press.

Jaiswal, P. K., Puri, S., & Das, S. K. (2012). Surface-directed spinodal decomposition: A molecular dynamics study. *Physical Review E, 85*, 051137. https://doi.org/10.1103/PhysRevE.85.051137

Kob, W., & Andersen, H. C. (1995). Testing mode-coupling theory for a supercooled binary Lennard–Jones mixture. *Physical Review E, 51*(5), 4626–4641. https://doi.org/10.1103/PhysRevE.52.4134

Laradji, M., Guo, H., Grant, M., & Zuckermann, M. J. (1997). Molecular dynamics study of spinodal decomposition in binary fluids. *Physical Review E, 55*(5), 5455–5460. https://doi.org/10.1103/PhysRevLett.77.2253

Lifshitz, I. M., & Slyozov, V. V. (1961). The kinetics of precipitation from supersaturated solid solutions. *Journal of Physics and Chemistry of Solids, 19*(1–2), 35–50. 10.1016/0022-3697(61)90054-3

Onuki, A. (2002). *Phase transition dynamics*. Cambridge University Press.

Siggia, E. D. (1979). Late stages of spinodal decomposition in binary mixtures. *Physical Review A, 20*(2), 595–605. https://doi.org/10.1103/PhysRevA.20.595

Thakre, A. K., den Otter, W. K., & Briels, W. J. (2008). Domain formation and growth in spinodal decomposition of a binary fluid by molecular dynamics simulations. *Physical Review E, 77*, 011503. https://doi.org/10.1103/PhysRevE.77.011503

Toxvaerd, S. (1994). Molecular dynamics simulation of phase separation in chemically reactive binary mixtures. *Molecular Physics, 81*(6), 1295–1310. https://doi.org/10.1103/PhysRevE.53.3710

Wagner, C. (1961). Theorie der Alterung von Niederschlägen durch Umlösen (Ostwald-Reifung). *Zeitschrift für Elektrochemie, 65*, 581–591. https://doi.org/10.1002/bbpc.19610650704